

Pathlength distributions of atmospheric neutrinos

T.K. Gaisser & Todor Stanev

Bartol Research Institute, University of Delaware, Newark, DE 19716

We present the distribution of the production heights of atmospheric neutrinos as a function of zenith angle and neutrino energy. The distributions can be used as the input for evaluation of neutrino propagation under various hypotheses for neutrino flavor oscillations.

I. INTRODUCTION

Initial results from SuperKamiokande [1] appear to confirm indications from IMB, [2] Kamiokande [3] and Soudan [4] of an excess of ν_e relative to ν_μ in the atmospheric neutrinos. One possible interpretation is that neutrino flavor oscillations play a role. In a two-flavor mixing scheme, for example, the probability that a neutrino of flavor i and energy E_i retains its identity after propagating a distance L in vacuum is [5]

$$P_{ii} = 1 - \sin^2 2\theta \sin^2 \left[\frac{1.27 \Delta m^2 (eV^2) \times L (km)}{E_i (GeV)} \right], \quad (1.1)$$

where δm^2 is the difference in mass squared of the two neutrino mass eigenstates and θ is the mixing angle. Therefore, to evaluate the manifestation of the mixing in a detector that measures to some degree the direction and energy of neutrino-induced events, one needs to know the distributions of production heights of the neutrinos as a function of energy and zenith angle. More complicated mixing schemes [6] and effects of propagation in matter [7] still require this basic information about the points of origin of the neutrinos.

Information about origin of the neutrinos is implicit in any calculation of neutrino fluxes. Here we extract the relevant information from the simulation of Ref. [8], which has been compared to several other calculations in Ref. [9].

The paper is organized in three sections. First we review the simulation we are using to calculate production of neutrinos in the atmosphere. Next we present the basic results of the calculation. We discuss simple analytic approximations which offer insight into the systematics of the results and compare them to simulation results for zenith angles from the vertical to horizontal. Finally, we provide some parametrizations, based on the analytic approximations, that may be useful for practical application of the results.

II. SIMULATION

The simulation was performed in the spirit of earlier calculations of the atmospheric neutrino flux [8,10]. The simulation code is one dimensional. In this approximation, all secondaries are assumed to move in the direction of the primary particles (except for a small fraction of low energy secondaries with angles larger than 90° to the beam, which are discarded). The validity of this approximation has been checked in Refs. [11,12].

The primary cosmic ray flux and its composition is the parametrization used previously in the calculation of Agrawal *et al.* [8] which in the multi-GeV range falls in between the measurements of Refs. [13,14]. Incident cosmic-ray nuclei are treated in the superposition approximation [15], with cascades generated separately for protons and neutrons in order to insure the correct ratios of neutrinos and antineutrinos. The fraction of neutrons is derived from the fractions of nuclei heavier than hydrogen in the primary flux.

We consider three ranges of neutrino energies that correspond approximately to the three major types of experimental events in a detector the size of SuperKamiokande: contained events; partially contained neutrino interactions and stopping neutrino induced muons; and throughgoing muons. The energy ranges are presented in two different ways:

- $0.3 < E_\nu < 2$ GeV; $2 < E_\nu < 20$ GeV; $E_\nu > 20$ GeV and
- $E > 1, 10$ and 100 GeV.

The integral form is more closely related to simple analytic approximations that we use as the basis of parametrizations of the results of Monte Carlo simulations.

Our results are obtained with the geomagnetic cutoffs for Kamioka and for the epoch of solar minimum, which is applicable to measurements performed currently ($\sim 1994 - 99$). Because of the high geomagnetic cutoffs at Kamioka,

it is not necessary to account precisely for the phase of the solar cycle. To illustrate the potential influence of geomagnetic effects at other locations we also tabulate some results for the much higher geomagnetic latitude of the SNO experiment.

We have not included prompt neutrino production through charm decay because it is totally negligible in the considered energy ranges [16,17]. All neutrinos are generated either in pion and kaon decays or in muon decays. The production heights are stored separately for neutrinos from π/K and from muon decays. The muon decay procedure accounts for the muon energy loss during propagation in the atmosphere. Technically the muon lifetime is sampled in the muon rest frame and then the muon is propagated in the atmosphere with time dilation proportional to its decreasing energy. Thus muons decay on the average sooner than they would have if one (incorrectly) sampled from a decay distribution using their Lorentz factor at production.

III. RESULTS

Before presenting the results for neutrinos, we show a comparison between measurements of GeV muons at different altitudes in the atmosphere and our calculation made with the same Monte Carlo code [19]. This type of balloon measurement provides the most direct test of the validity of the cascade model and of the treatment of the muon propagation in the atmosphere because the muons and neutrinos have a common origin. The comparison shown in Fig. 1 is with data of the MASS experiment [18] as discussed in Ref. [19].

Fig. 2 shows the height of production of neutrinos of energy above 1 GeV for $\cos(\theta) = 0.75$. The graph gives dN_ν/dh ($\text{cm}^{-2}\text{s}^{-1}\text{sr}^{-1}\text{km}^{-1}$), where h is the slant distance from the neutrino production point to sea level. Contributions from muon decay and from π/K decay are shown separately for $\nu_e + \bar{\nu}_e$ and for $\nu_\mu + \bar{\nu}_\mu$. The overall flux of $\nu_e + \bar{\nu}_e$ from π/K decay is much lower because it reflects primarily the contribution of K_L^0 decays, which is very low in this energy range. The curves for electron and for muon neutrinos from muon decay are nearly equal. They extend to lower altitudes with a slope that depends on the average energy of the parent muons. For higher energy neutrinos this slope is significantly flatter as a consequence of the higher parent muon energy and correspondingly longer muon decay length. For $E_\nu > 20$ GeV, most parent muons reach the ground (except in nearly horizontal direction) and stop before decaying. As a consequence, the height distributions for neutrinos from muon decay deep in the atmosphere are nearly flat.

A. Height distribution for neutrinos from π/K decay

1. Analytic approximation

It is instructive to look at a simple approximation for the height of production of neutrinos from decay of pions. In the approximation of an exponential atmosphere with scale height h_0 and the approximation of Feynman scaling for the production cross sections of pions in interactions of hadrons with nuclei of the atmosphere, a straightforward solution of the equations for propagation of hadrons through the atmosphere [20] gives [21]

$$\frac{dF(> E_\nu)}{dX} = (1 - r_\pi)^{-\gamma} \frac{Z_{N\pi}}{\lambda_N} e^{-X/\Lambda_N} \frac{K}{\gamma(\gamma + 1)} E_\nu^{-\gamma} \equiv A \times E_\nu^{-\gamma} \quad (3.1)$$

for the integral flux of neutrinos in the energy range $E_\nu \ll \epsilon_\pi$ where reinteraction of pions in the atmosphere can be neglected. There is a similar expression for neutrinos from decay of kaons proportional to $B_K \times Z_{NK}$. The meaning and approximate values of the quantities in these equations are given in Table I.

TABLE I. Values of the parameters used in Eq. 3.1 that correspond to a power law primary cosmic ray spectrum and to an exponential atmosphere. γ and K are the spectral index and the coefficient of the differential cosmic ray energy spectrum, $dN/dE = KE^{-(\gamma+1)}$. r_π (r_K) is $(m_\mu/m_\pi)^2$ ($(m_\mu/m_K)^2$). $Z_{N\pi}$ (Z_{NK}) is the spectrum weighted moment for pion (kaon) production by nucleons ($Z_{N\pi} = \int dx x^\gamma dN/dx$). Λ_N and λ_N are the attenuation and interaction lengths for nucleons. B_K is the branching ratio for $K \rightarrow \mu$ decay. X_0 and h_0 are the total vertical thickness (in g/cm^2) and the scaleheight for an exponential atmosphere in km.

γ	K $\text{cm}^{-2}\text{s}^{-1}\text{sr}^{-1}(\text{GeV})^\gamma$	λ_N g/cm^2	Λ_N g/cm^2	$Z_{N\pi}$	$B_K \times Z_{NK}$	r_π	r_K	X_0 g/cm^2	h_0 km
1.70	1.8	86	120	0.08	0.0075	0.5731	0.0458	1030	6.4

In Eq. 3.1 X is the slant depth in the atmosphere at which the pion is produced and decays. We now convert this into distance ℓ from the detector in the approximation of an exponential atmosphere in which

$$X = \frac{X_0}{\cos \theta} \exp \left[-\frac{\ell \cos \theta}{h_0} \right]. \quad (3.2)$$

For $\theta < 70^\circ$, curvature of the earth can be neglected and $\cos \theta$ in Eq. 3.2 is cosine of the zenith angle to a good approximation. The effective values of $\cos \theta$ for larger angles are given below.

The corresponding approximate expression for the distribution of production distances is

$$\frac{dF(> E_\nu)}{d\ell} = \frac{AX_0}{h_0} E_\nu^{-\gamma} \exp \left[-\frac{X}{\Lambda_N} \right] \times \exp \left[-\frac{\ell \cos \theta}{h_0} \right], \quad (3.3)$$

where X is to be evaluated as a function of ℓ from Eq. 3.2. Assuming a primary cosmic ray nucleon flux with the normalization given in Table I (and including the small contribution from decay of kaons) the normalization factor is $AX_0/h_0 \simeq 0.020$.

Taking parameters from Table I gives the most probable distance of production as

$$\ell_{max} \approx \frac{h_0}{\cos \theta} \ln \frac{X_0}{\Lambda_N \cos \theta}, \quad (3.4)$$

which is ≈ 15 km for vertical neutrinos from decay of pions.

2. Monte Carlo results

Fig. 3 shows the distance distribution for neutrinos from π/K decay ($E_\nu > 1$ GeV) for $\cos(\theta) = 1.00, 0.75, 0.50, 0.25, 0.15$ and 0.05 . Here θ is the zenith angle of the neutrino trajectory at the surface of the Earth. For large zenith angles, the curvature of the Earth is significant, and it is necessary to use effective values of $\cos_{eff}(\theta)$ that represent the convolution of the locations of neutrino production with the local zenith angle as it decreases moving upward along the trajectory. We treat $\cos_{eff}(\theta)$ as a free parameter in fitting Eqs. 3.3 and 3.5 to the Monte Carlo results. The values are included in Table II.

TABLE II. Comparison of analytic and Monte Carlo values of the effective value of $\cos \theta$. Column 1 shows the cosine of the zenith angle θ . Column 2 shows the most probable production height for neutrinos from π/K decay from the Monte Carlo calculation. Column 3 gives the most probable height of production from Eq. 3.4 with $\cos_{eff}\theta$ from column 4. Columns 4 & 5 give the $\cos_{eff}\theta$ values that fit best the calculated height of production distributions for neutrinos from π/K and muon decay with $h_0 = 6.50$ km. Column 6 gives the normalization coefficient C_μ needed to fit the distribution for neutrinos from muon decay.

$\cos \theta$	$\ell_{max}(MC)$ (km)	$\ell_{max}(\text{Eq. 3.4})$ (km)	$\cos_{eff}^{K/\pi} \theta$	$\cos_{eff}^\mu \theta$	C_μ
1.00	13.8	14.0	1.00	1.00	0.69
0.75	21.6	21.2	0.75	0.75	0.71
0.50	38.4	37.0	0.50	0.50	0.77
0.25	88.4	87.5	0.26	0.26	0.83
0.15	155.	157.	0.164	0.168	1.00
0.05	382.	358.	0.084	0.087	1.86

Up to $\cos \theta = 0.25$ the agreement between the Monte Carlo calculation and the analytic estimate is quite good. Note that for nearly horizontal neutrinos the height distribution from the Monte Carlo calculation is artificially narrow and irregular. The atmospheric model used does not treat exactly the atmospheric densities at vertical depths of less than few g/cm^2 . This intruduces a sharp cutoff in the height distribution for strongly inclined showers and also decreases the width of the height distribution.

The height distribution of ν_e from π/K decay has a similar shape with much lower normalization, because only K_L^0 have decay mode with ν_e 's (K_{e3}^0).

B. Height distribution for neutrinos from muon decay

1. Analytic approximation

To estimate the height of production for neutrinos from decay of muons is more complicated because of the competition between decay and energy loss for muons in the multi-GeV energy range. One starts from the distribution of production points for muons, which is similar to Eq. 3.1 with different coefficients. The resulting approximate expression [21] for the distribution of production distances (differential in the energy of the parent muons as well as the slant height of production) is

$$\frac{dN_\nu}{dE_\mu d\ell} = KB \frac{\mu c^2}{E_\mu c\tau} \int_0^X \frac{dY}{\lambda_N} \frac{e^{-Y/\Lambda_N} \left[\frac{X}{Y} \frac{E_\mu + \alpha(X-Y)}{E_\mu} \right]^{-p}}{[E_\mu + \alpha(X-Y)]^{\gamma+1}}, \quad (3.5)$$

where τ is the muon lifetime,

$$p = \frac{h_0}{c\tau \cos \theta} \frac{\mu c^2}{E_\mu + \alpha X}$$

and

$$B = \frac{1}{\gamma+1} \left[\frac{1 - r_\pi^{(\gamma+1)}}{1 - r_\pi} Z_{N\pi} + B_K \frac{1 - r_K^{(\gamma+1)}}{1 - r_K} Z_{NK} \right].$$

At high altitude muon energy loss ($\alpha(X - Y)$) can be neglected and the expression 3.5 is proportional to slant depth X given by Eq. 3.2. This expression gives a good account of the high-altitude exponential falloff of the neutrinos from muon decay.

An approximation that is adequate for fitting the distribution for all distances (integrated over neutrino energy) is

$$\frac{dN_\nu(> E_\nu)}{d\ell} \approx \frac{C_\mu KB}{(\gamma+1)(2E_\nu)^{\gamma+1}} \frac{\mu c^2}{c\tau} \frac{X}{\lambda_N} \int_0^1 dz z^p \exp\left(-\frac{X}{\Lambda_N} z\right) \left[1 + \frac{\alpha X}{2E_\nu}(1-z)\right]^{-(p+\gamma+1)}, \quad (3.6)$$

where C_μ is an overall normalization factor used to fit the Monte Carlo results (see Table II).

2. Monte Carlo results

Fig. 4 shows the height of production distributions for muon neutrinos of energy above 1 GeV from muon decay. The lines are calculated according to Eq. 3.6 with values of $\cos_{eff} \theta$ as given in Table II. To obtain the fits shown in Fig. 4 the approximations of Eq. 3.6 have also been renormalized as indicated in Table II.

At high altitude the height of production distributions have the same shape as the ones from neutrinos from π/K decay, shifted to lower altitudes by one muon decay length (6.24 km for 1 GeV muons). At lower altitude the shapes are quite different. The production height for neutrinos from muon decay extend to much lower altitude because of the slow attenuation of the parent muon flux, an effect which becomes more pronounced as the energy increases.

It is interesting to observe that at high zenith angles the yield of neutrinos from (daughter) muon decay exceeds the yield of neutrinos from the decay of the parent pions and kaons. The reason is that muon neutrinos from muon decay in flight have a spectrum extending almost to $x = 1$ (where $x = E_\nu/E\pi$), while the neutrinos from π decay can only reach $E_\nu^{max} = E_\pi \times (1 - r_\pi) = 0.428 E_\pi$. The corresponding Z -factors $Z_{\pi\nu_\mu}$ and $Z_{\pi\nu_e}$ are 0.133 and 0.087 respectively, including the effect of muon polarization in pion decay. The result is that for large zenith angles, when almost all muons decay the ν_μ yield from muon decay becomes slightly larger than that from π/K decay ($\sim 9/7$ for $\cos \theta = 0.05$).

Fig. 5 compares the distributions of distance to production for ν_μ from muon decay with E_ν above 1, 10, and 100 GeV. At high neutrino energy the muon decay length becomes comparable or larger than the total dimension of the atmosphere. The neutrino height of production then becomes constant deep in the atmosphere.

The height distribution for ν_e from muon decay is analogous to that of ν_μ . The only difference is the slightly lower normalization, which reflects the ratio $Z_{\mu\nu_\mu}/Z_{\mu\nu_e} = 0.133/0.129 = 1.03$ (including muon polarization).

C. Height distribution in three energy bins

In Table III we show the average height of production and the contributions of π/K and muon decays for neutrinos in the three energy bins ($0.3 < E_\nu < 2$ GeV; $2 < E_\nu < 20$ GeV; $E_\mu > 20$ GeV) which roughly correspond to contained neutrino events, semicontained events and stopping neutrino induced muons and throughgoing neutrino induced muons. For each angle and neutrino flavor Table III first gives the average height of production (slant depth) in km and the width of the height of production distribution. Then it gives the contribution (in %) of π/K decay f_m and the corresponding $\langle h_m \rangle$ and σh_m , then the same quantities (f_μ , $\langle h_\mu \rangle$, σh_μ) for neutrinos from muon decay.

The calculation was done with the geomagnetic cutoffs of Kamioka, except for the three lines ($\cos\theta = 1.00, 0.75$ and 0.50 , for the lowest energy bin) that are also calculated for the high geomagnetic latitude of SNO [22]. The numbers for high geomagnetic latitude are slightly higher (2 – 10 %) for both neutrino sources because of the contribution of low energy protons. This difference becomes negligible at higher angles.

TABLE III. Production height (slant distance, km) of neutrinos for six values of $\cos\theta$ and three neutrino energy ranges. The calculation is for the geomagnetic location of Kamioka with three lines for the lowest energy range calculated for Sudbury, Canada.

E, GeV $\cos\theta$	$\nu_e + \bar{\nu}_e$									$\nu_\mu + \bar{\nu}_\mu$								
	h	σ_h	$f_{\pi/K}$	$h_{\pi/K}$	$\sigma h_{\pi/K}$	f_μ	h_μ	σh_μ	h	σ_h	$f_{\pi/K}$	$h_{\pi/K}$	$\sigma h_{\pi/K}$	f_μ	h_μ	σh_μ		
0.3 – 2.																		
1.00	14.0	8.7	1.3	16.8	8.3	98.7	14.0	8.7	15.9	8.7	57.4	17.4	8.4	42.6	14.1	8.7		
0.75	21.0	11.9	1.2	25.6	11.9	98.8	21.0	11.9	23.6	11.8	54.5	25.6	11.4	45.5	21.1	11.9		
0.50	37.7	18.4	1.0	44.0	17.2	99.0	37.6	18.3	41.0	18.1	51.3	44.0	17.2	48.7	37.8	18.3		
0.25	91.1	32.0	0.9	100.5	29.9	99.1	90.9	32.1	95.6	31.4	48.7	100.2	30.2	51.3	91.3	32.0		
0.15	154.8	38.1	0.9	167.6	35.1	99.1	154.6	38.2	160.0	37.3	47.9	165.6	35.3	52.1	155.0	38.0		
0.05	363.8	56.5	0.9	378.0	52.8	99.1	363.7	56.5	369.8	55.0	47.4	376.1	53.1	52.6	364.1	56.3		
SNO																		
1.00	15.4	8.9	0.8	17.2	8.6	99.2	15.4	8.9	16.9	8.8	53.8	18.0	8.5	46.2	15.5	8.9		
0.75	23.2	12.1	0.7	25.6	11.3	99.3	23.2	12.1	25.0	11.9	51.1	26.5	11.5	48.9	23.3	12.1		
0.50	40.6	18.4	0.6	44.4	17.3	99.4	40.6	18.4	43.0	18.1	48.3	45.2	17.4	51.7	40.8	18.3		
2. – 20.																		
1.00	13.4	9.1	6.7	17.9	8.9	93.3	13.1	9.0	16.6	9.0	71.6	18.0	8.6	28.4	13.1	8.9		
0.75	19.6	12.4	5.4	26.3	11.6	94.6	19.3	12.3	24.1	12.1	67.0	26.4	11.4	33.0	19.4	12.3		
0.50	34.4	19.6	3.9	44.8	17.4	96.1	34.0	19.5	40.9	19.1	60.2	45.3	17.5	39.8	34.2	19.3		
0.25	81.9	35.6	2.9	102.8	31.1	97.1	81.3	35.6	92.8	34.6	52.6	102.9	30.5	47.4	81.7	35.4		
0.15	139.5	45.2	2.5	168.6	34.9	97.5	138.8	45.2	154.3	42.8	49.2	169.1	35.0	50.8	139.9	44.9		
0.05	338.9	73.0	2.2	380.6	51.5	97.8	338.0	73.1	359.0	67.1	46.2	381.6	52.0	53.8	339.5	72.4		
> 20.																		
1.00	14.0	9.3	41.5	17.7	8.7	58.5	11.4	8.9	17.6	8.9	94.2	17.9	8.7	5.8	11.6	9.1		
0.75	20.0	13.1	33.1	26.4	11.7	66.9	16.8	12.6	25.8	12.1	91.9	26.6	11.7	8.1	16.6	12.4		
0.50	31.8	20.3	22.3	44.8	17.7	77.7	28.0	19.4	43.3	18.9	87.8	45.4	17.8	12.2	28.0	19.4		
0.25	70.3	38.9	7.8	99.1	27.2	92.2	67.2	38.6	94.9	36.4	79.6	103.8	29.9	20.4	60.1	39.5		
0.15	110.3	54.7	8.8	168.1	35.0	91.2	104.7	53.0	151.2	49.4	72.5	168.7	34.6	27.5	105.2	52.7		
0.05	267.4	105.1	5.4	382.1	54.8	94.6	260.8	103.5	335.7	94.2	61.7	381.7	51.1	38.3	262.3	100.5		

There are two obvious trends in the numbers in Table III. The height of production for neutrinos from π/K decay grows slightly with the neutrino energy because higher energy mesons preferentially decay (rather than interact) in the tenuous atmosphere at high altitude. Neutrinos from muon decay, on the other hand, are generated at lower altitude at high energy because of the increasing muon decay length. This second feature is much stronger because of the proportionality of decay length and muon energy.

The average heights of production also reflect the relative yields of the two neutrino sources. For low energy $\nu_e(\bar{\nu}_e)$, for example, the contribution of K_{e3}^0 is small, so the average height of production is dominated by muon decay. At higher energy the relative contribution of K_{e3}^0 grows, especially at directions close to the vertical, and $\langle h \rangle$ becomes intermediate between those of the two processes with correspondingly larger width.

Generally the contribution from muon decay increases significantly with the zenith angle since even 20 GeV muons easily decay in cascades developing in nearly horizontal direction.

IV. CONCLUSIONS

We have calculated the distribution of pathlengths of atmospheric neutrinos for a range of angles and energies relevant for current searches for neutrino oscillations with atmospheric neutrinos. Accounting correctly for the pathlength will be particularly important for neutrinos near the horizontal direction where the pathlength through the atmosphere of neutrinos from above the horizon is of the same order of magnitude as the pathlength through the Earth of neutrinos from below the horizon. We have also given simple approximations that may be useful in interpolating the tables and adapting the results for different energy ranges and directions.

The influence of the geomagnetic effects on the calculated height of neutrino production distributions is not very strong. The difference in the average production heights for neutrinos detected at Kamioka and SNO is of order several per cent in directions relatively close to the vertical. This difference diminishes with angle and becomes totally negligible for upward going neutrinos, where the geomagnetic cutoffs becomes approximately equal, being averaged over the geomagnetic fields of the opposite hemisphere.

The agreement of our calculation with the measured muon fluxes above 1 GeV/c as a function of the atmospheric depth serves as a check on the validity of the results presented above.

ACKNOWLEDGMENTS

The authors express their gratitude to W. Gajewski, J.G. Learned, H. Sobel, and Y. Suzuki for their interest in the height of production problem that inspired us to complete this research. This work is supported in part by the U.S. Department of Energy under DE-FG02-91ER40626.A007.

-
- [1] Z. Conner, Hightlight talk at the 25th International Cosmic Ray Conf. (Durban, South Africa, 1997) to be published; J.G. Learned (SuperKamiokande Collaboration), *Proc. 25th International Cosmic Ray Conference*, eds. M.S. Potgieter, B.C. Raubenheimer and D.J. van der Walt, **7**, 73 (1997).
 - [2] R. Becker-Szendy *et al.*, (IMB Collaboration), *Phys. Rev.* **D46** (1992) 3720. See also D. Casper *et al.* *Phys. Rev. Letters*, **66** (1991) 2561.
 - [3] K.S. Hirata *et al.*, (Kam-II Collaboration), *Phys. Letters*, **B280** (1992) 146 and Y. Fukuda *et al.*, *Phys. Letters*, **B335** (1994) 237.
 - [4] M.C. Goodman *et al.*, (Soudan 2 Collaboration), *Proc. 25th International Cosmic Ray Conference*, eds. M.S. Potgieter, B.C. Raubenheimer and D.J. van der Walt, **7**, 77 (1997).
 - [5] *Physics of Massive Neutrinos*, by Felix Boehm & Peter Vogel (Cambridge University Press, 1992).
 - [6] G.L. Fogli and E. Lisi, *Phys. Rev.* , **D52** (1995) 2775.
 - [7] R.H. Bernstein & S. Parke, *Phys. Rev. D*, **44**, 2059 (1991).
 - [8] V. Agrawal *et al.*, *Phys. Rev.* **D53** (1996), 1314.
 - [9] T.K. Gaisser *et al.*, *Phys. Rev.* **D54** (1996) 5578.
 - [10] Giles Barr, T.K. Gaisser & Todor Stanev, *Phys. Rev.* **D39** (1989) 3532.
 - [11] H. Lee & S.A. Bludman, *Phys. Rev.* **D37** (1988) 122.
 - [12] T.K. Gaisser & Todor Stanev, *Proc. 24th ICRC (Rome)* vol. 1, p. 694.
 - [13] W.R. Webber, R.L. Golden and S.A. Stephens, in *Proc. 20th Int. Cosm. Ray Conf. (Moscow)* **1**, 325 (1987).
 - [14] E.-S. Seo *et al.* *Ap. J.* **378**, 763 (1991).
 - [15] J. Engel *et al.* *Phys. Rev.* **D46**, 5013 (1992).
 - [16] M. Thunmann, G. Ingelman & P. Gondolo, *Astropart. Physics* **5** (1996) 309.
 - [17] L.V. Volkova, W. Fulgione, P. Galeotti & O. Saavedra, *Nuovo Cimento* **C10** (1987) 465.
 - [18] R. Bellotti *et al.*, *Phys. Rev.* **D53**, 35 (1996).
 - [19] Marco Circella, Carlo De Marzo, T.K. Gaisser & Todor Stanev, *Proc. 25th Int. Cosmic Ray Conf. (Durban)* **7**, 117 (1997).
 - [20] *Cosmic Rays and Particle Physics*, by Thomas K. Gaisser, (Cambridge University Press, 1990).
 - [21] Paolo Lipari, *Astroparticle Physics* **1**, 195 (1993).
 - [22] M.E. Moorhead (for the SNO Collaroration), *Nucl. Phys. B (Proc. Suppl.)* **48** 378 (1995).

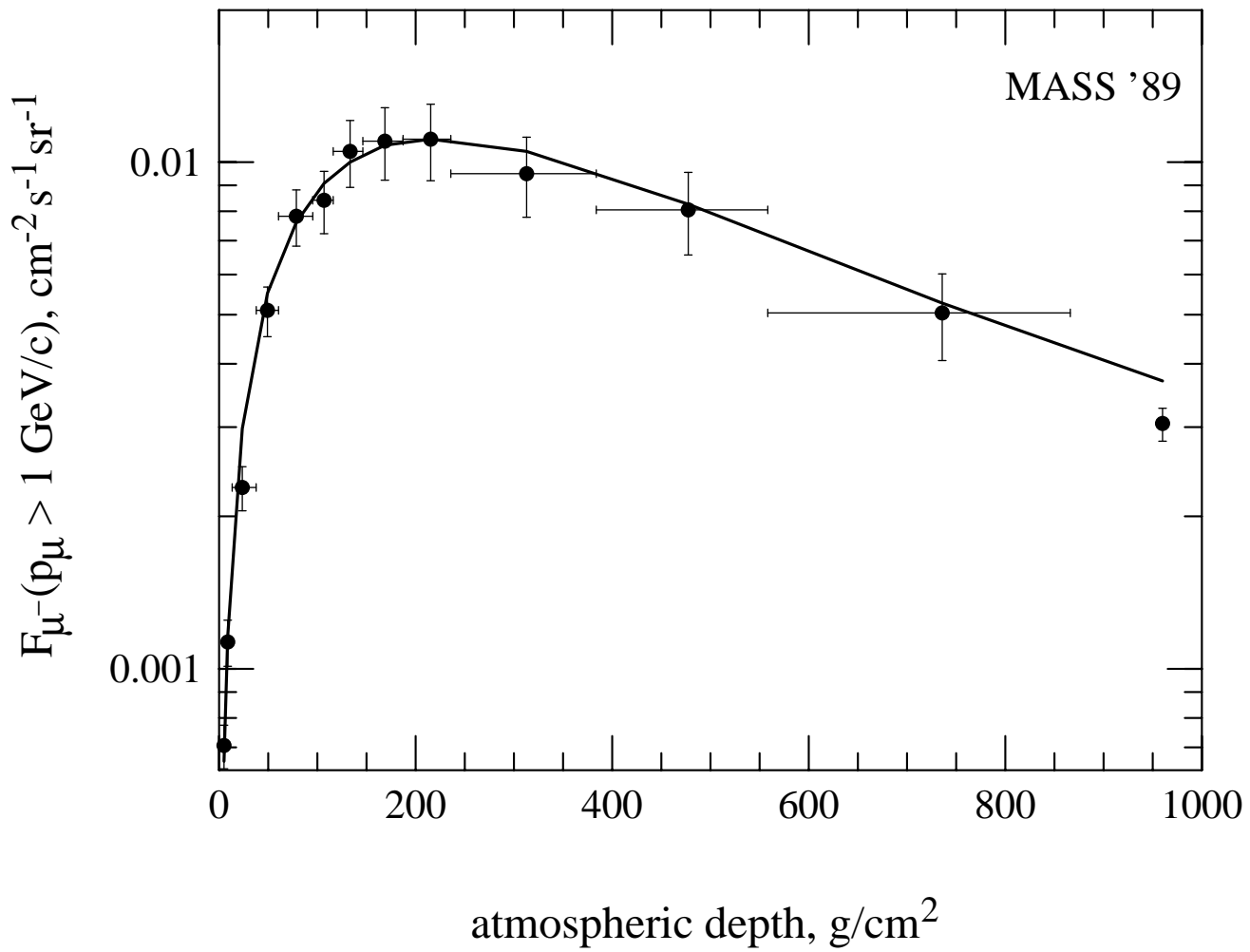
FIG. 1. Comparison of the calculated flux of negative muons above 1 GeV/c as a function of the atmospheric depth to the measurements of the MASS experiment. [18,19]

FIG. 2. Height of production distribution for neutrinos of energy above 1 GeV at $\cos\theta = 0.75$. The contributions of π/K and muon decays for the two neutrino flavors are clearly visible. Dots show the height of production for electron neutrinos from π/K decay, short dashes: $\nu_e + \bar{\nu}_e$ from muon decay. The heavy dash line is the sum of the two. Dash dot: $\nu_\mu + \bar{\nu}_\mu$ from π/K decay, dash–dash: $\nu_\mu + \bar{\nu}_\mu$ from muon decay. The heavy solid line is the sum of these two.

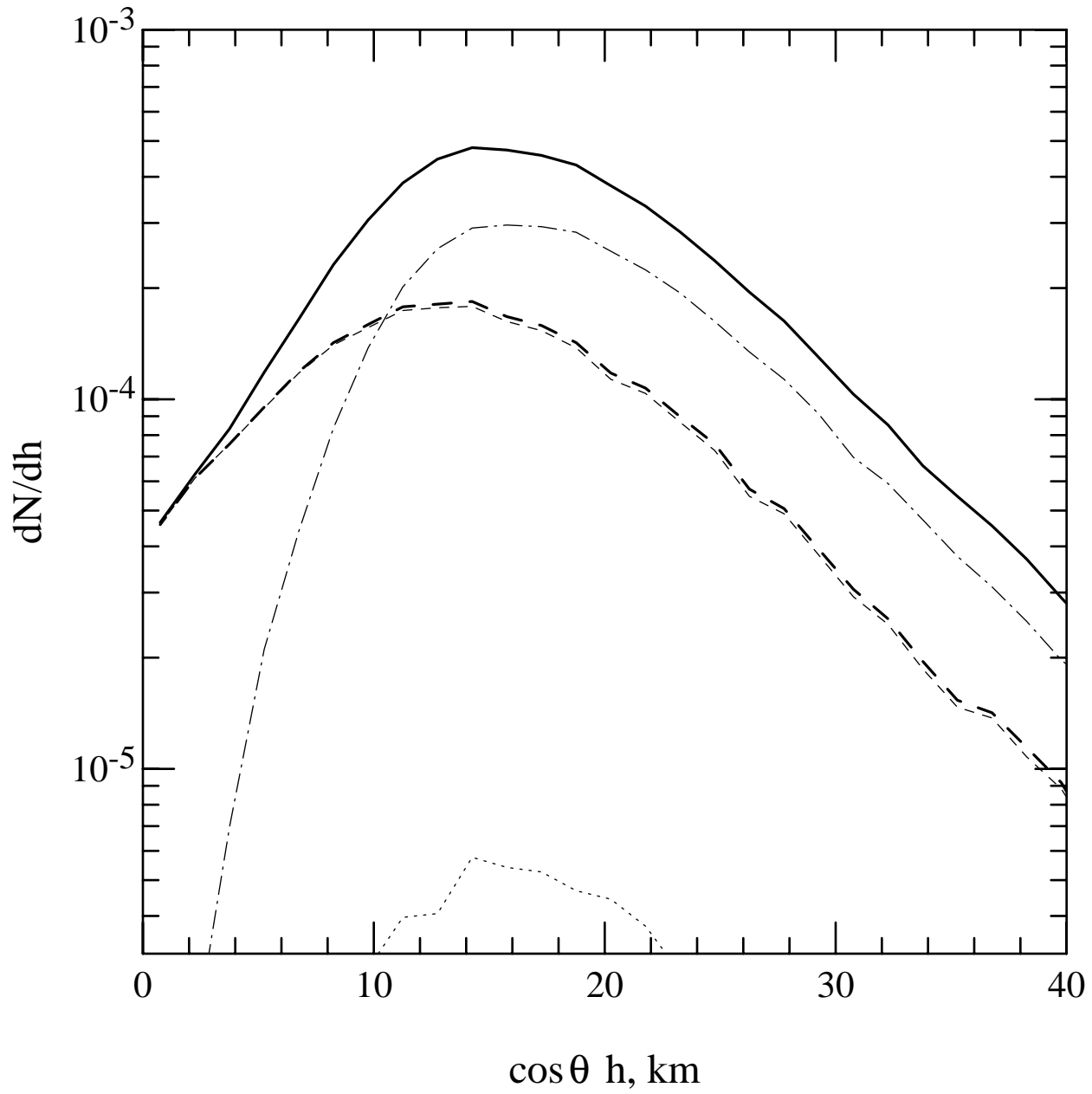
FIG. 3. Height of production for muon neutrinos above 1 GeV from π/K decay as a function of angle with different symbols. Lines show the best fits of Eq. 3.3 with the parameters given in Table II.

FIG. 4. Height of production for muon neutrinos above 1 GeV from muon decay as a function of angle (dots). Lines show the best fits of Eq. 3.6 with the parameters given in Table II.

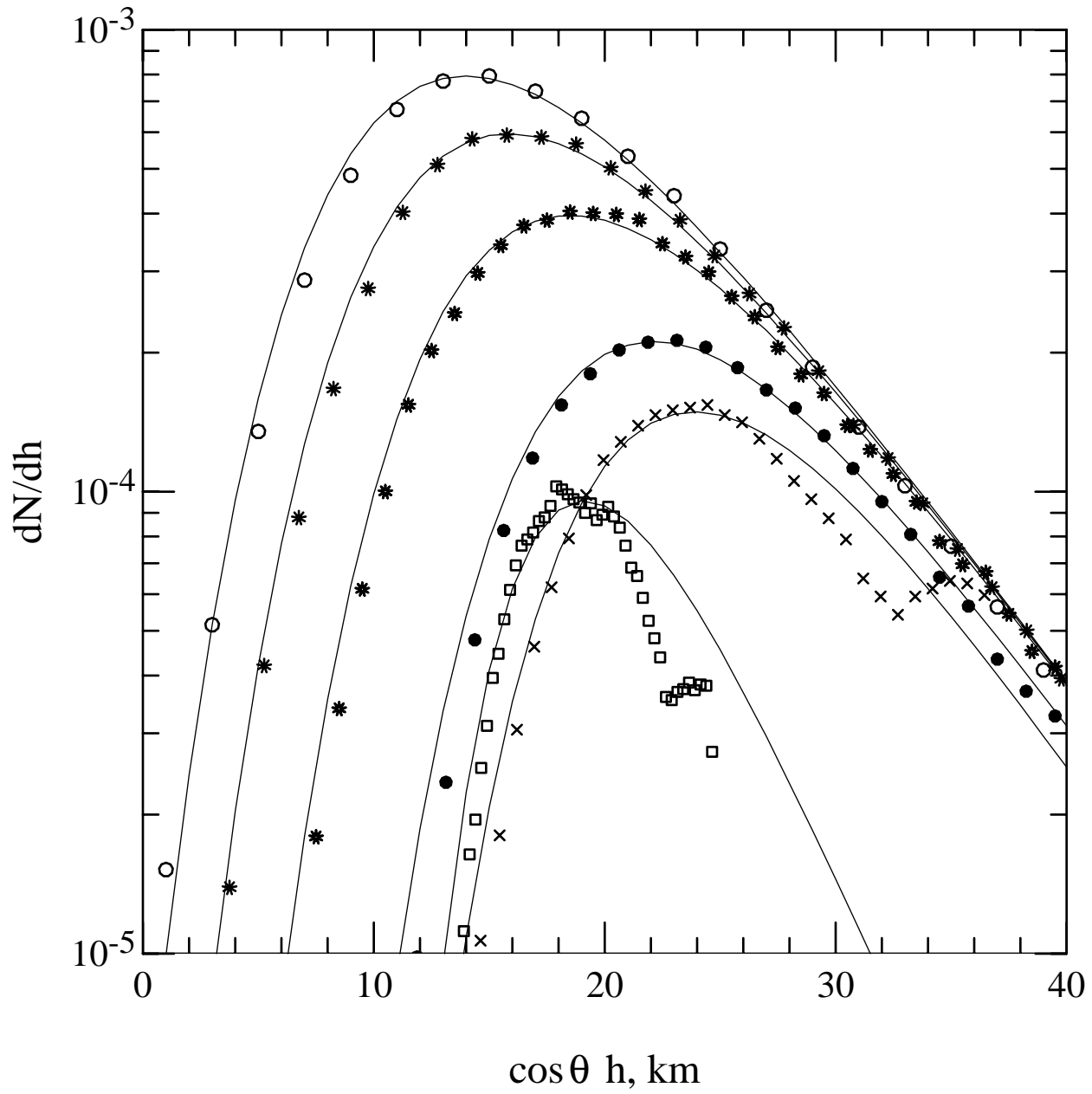
FIG. 5. Height of production for muon neutrinos above 1, 10, and 100 GeV from muon decay at $\cos\theta = 0.25$. Lines show the best fits of Eq. 3.6 and with normalization factors of 0.83, 0.50, and 0.33 for 1, 10, and 100 GeV respectively.



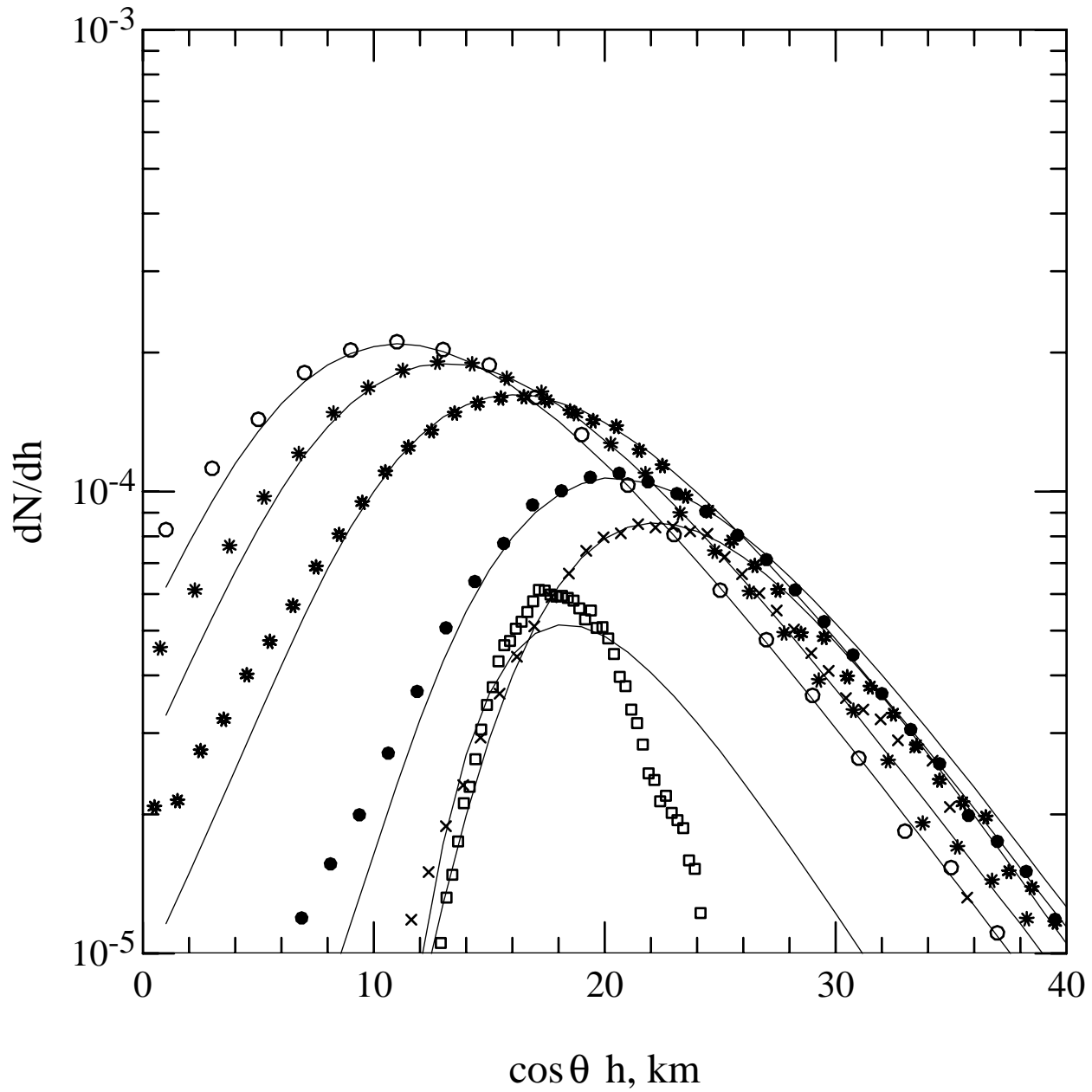
Gaisser & Stanev, "Height of production", Fig.1



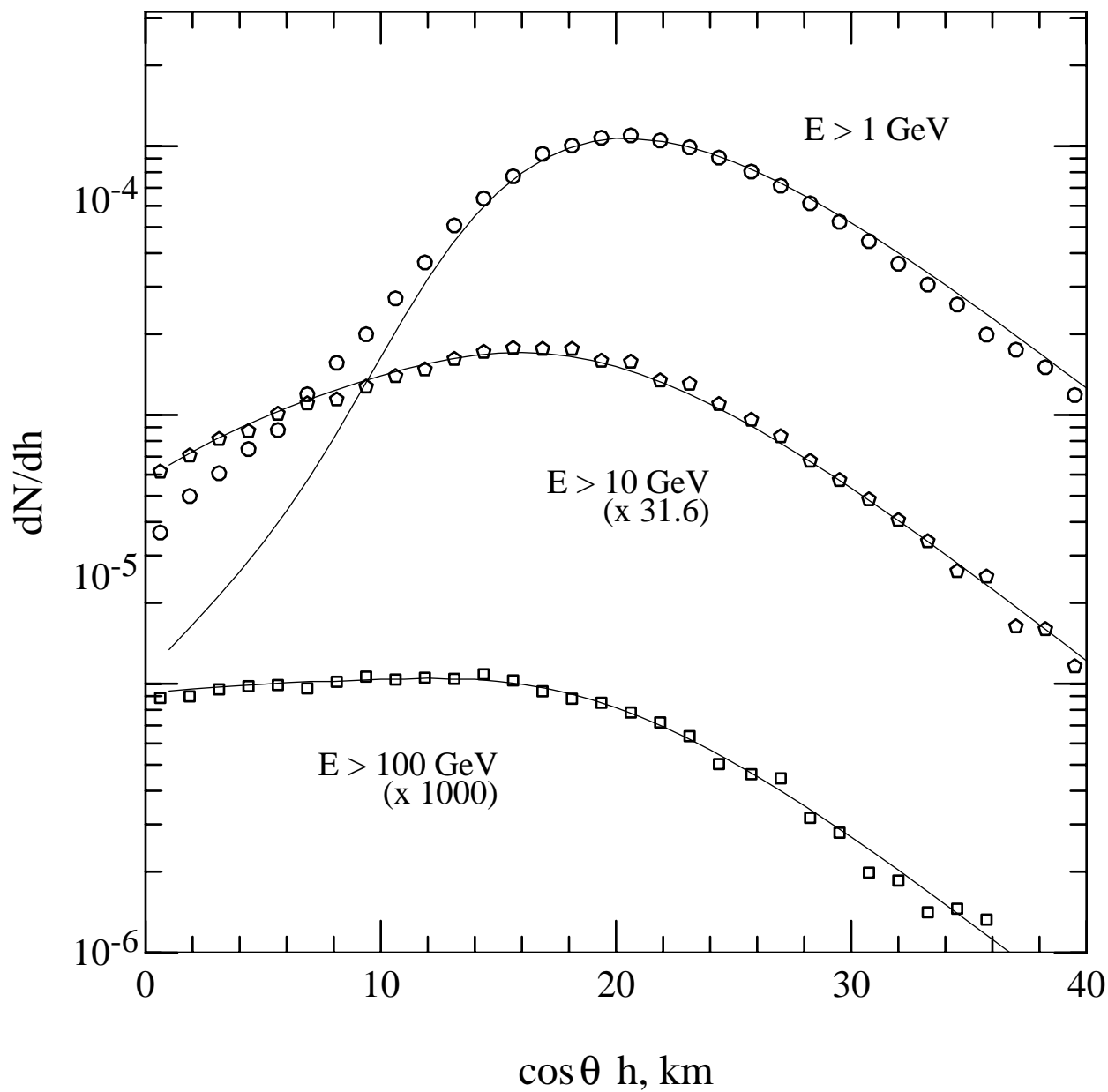
Gaisser & Stanev, "Height of production", Fig.2



Gaisser & Stanev, "Height of production", Fig.3



Gaisser & Stanev, "Height of production", Fig.4



Gaisser & Stanev, "Height of production", Fig.5